JACS
JOURNAL OF THE AMERICAN CHEMICAL SOCIETY
Article
pubs.acs.org/JACS

X-ray Crystallographic Structure of Oligomers Formed by a Toxic β-Hairpin Derived from α-Synuclein: Trimers and Higher-Order Oligomers

Patrick J. Salveson, Ryan K. Spencer, and James S. Nowick*

Department of Chemistry, University of California Irvine, Irvine, California 92697-2025, United States

Supporting Information

ABSTRACT: Oligomeric assemblies of the protein α-synuclein are thought to cause neurodegeneration in Parkinson's disease and related synucleinopathies. Characterization of α-synuclein oligomers at high resolution is an outstanding challenge in the field of structural biology. The absence of high-resolution structures of oligomers formed by α-synuclein impedes understanding the synucleinopathies at the molecular level. This paper reports the X-ray crystallographic structure of oligomers formed by a peptide derived from residues 36−55 of α-synuclein. The peptide **1a** adopts a β-hairpin structure, which assembles in a hierarchical fashion. Three β-hairpins assemble to form a triangular trimer. Three copies of the triangular trimer assemble to form a basket-shaped nonamer. Two nonamers pack to form an octadecamer. Molecular modeling suggests that full-length α-synuclein may also be able to assemble in this fashion. Circular dichroism spectroscopy demonstrates that peptide **1a** interacts with anionic lipid bilayer membranes, like oligomers of full-length α-synuclein. LDH and MTT assays demonstrate that peptide **1a** is toxic toward SH-SY5Y cells. Comparison of peptide **1a** to homologues suggests that this toxicity results from nonspecific interactions with the cell membrane. The oligomers formed by peptide **1a** are fundamentally different than the proposed models of the fibrils formed by α-synuclein and suggest that α-Syn$_{36-55}$, rather than the NAC, may nucleate oligomer formation.

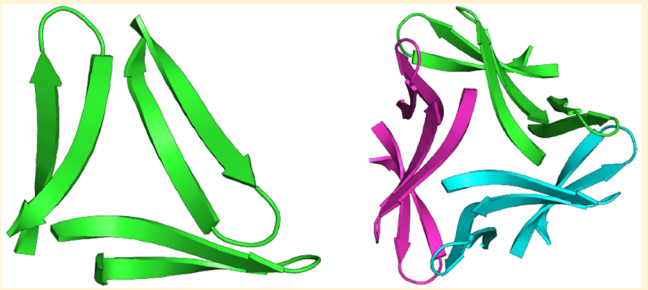

INTRODUCTION

Parkinson's disease is one of several amyloid disorders, collectively referred to as synucleinopathies, whose pathology is characterized by the aggregation of the presynaptic protein α-synuclein (α-Syn) into Lewy bodies.[1−3] Despite the appearance of these Lewy bodies in diseased brains, soluble oligomers of α-Syn seem to be the toxic agent in Parkinson's disease.[4] The characterization of α-Syn oligomers is an outstanding biophysical challenge due to their heterogeneity and propensity to aggregate. These properties have precluded α-Syn oligomers from high-resolution structural characterization by X-ray crystallography and have limited their characterization to a range of low-resolution techniques, including size-exclusion chromatography, SDS-PAGE, dynamic light scattering, analytical ultracentrifugation, and cryo-TEM.[5] The same properties have precluded oligomers formed by many amyloidogenic proteins from structural characterization at high resolution.

Small peptides derived from amyloidogenic proteins have afforded high-resolution structures that provide insights into the structures of amyloid oligomers formed by full-length proteins.[6−15] Studying the assembly of small peptides derived from α-Syn may provide insights into oligomeric assemblies of the protein. Several structural studies of α-Syn oligomers have suggested that two β-strands loosely defined by residues 36−43 and 49−58 form the core of the toxic oligomers associated with Parkinson's disease.[16−18] Most notably, Hoyer et al. recently observed a β-hairpin defined by residues 36−55 in monomeric α-Syn by NMR spectroscopy (Figure 1A).[19] The authors found that sequestering this β-hairpin in an engineered binding protein markedly reduces the toxicity of aged α-Syn and inhibits its fibrillization. The β-hairpin has also been observed in solution by others.[20,21]

Five of the six known disease-causing point mutations of Parkinson's disease are located within this β-hairpin, further emphasizing the importance that this region plays in the pathology of Parkinson's disease.[22−27] Recently, Schulten et al. have found through molecular dynamics simulations that residues 36−55 adopt a β-hairpin similar to that observed by Hoyer et al.[28] The authors also found that disease-causing point mutations stabilize the β-hairpin. They further suggest that β-hairpin formation precedes aggregation of α-Syn in the pathway to pathology. The concurrence of genetic and structural evidence motivated us to design a macrocyclic β-sheet that mimics this β-hairpin, with the goal of creating a high-resolution structural model of α-Syn oligomers (Figure 1).

We designed macrocyclic β-sheet peptide **1a** to mimic the β-hairpin formed by α-Syn$_{36-55}$ (Figure 1B and C): We incorporated the heptapeptides α-Syn$_{36-42}$ (GVLYVGS) and α-Syn$_{49-55}$ (VHGVATV) into the top and bottom strands of the

Received: December 18, 2015
Published: February 29, 2016

DOI: 10.1021/jacs.5b13261
J. Am. Chem. Soc. 2016, 138, 4458−4467

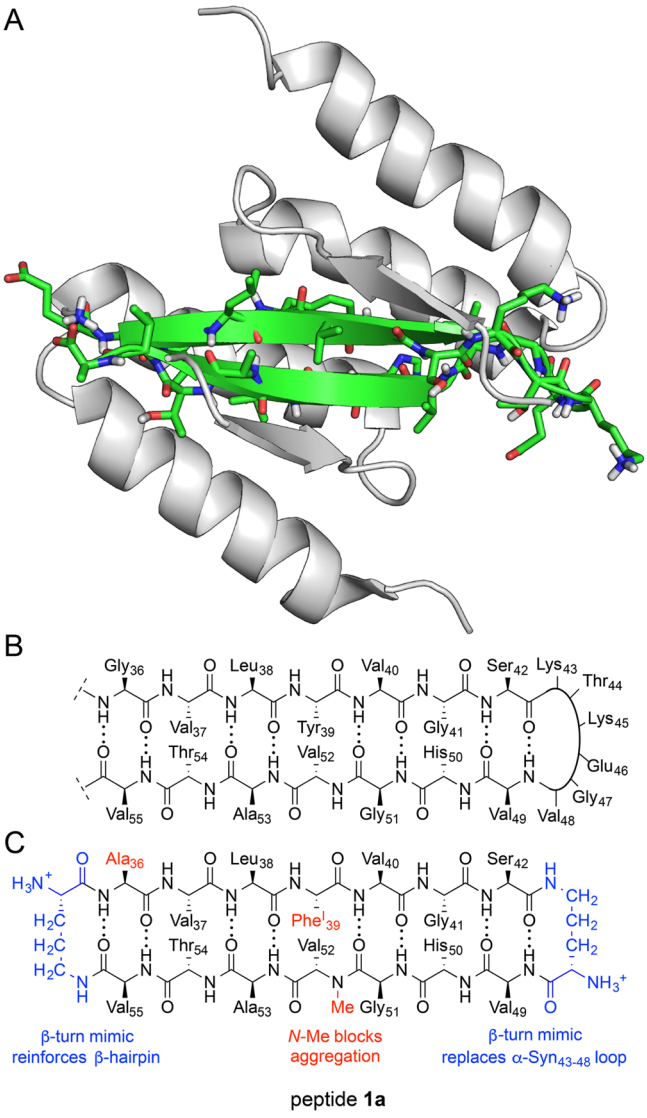

Figure 1. Design of peptide **1a**. (A) NMR structure of the β-hairpin formed by residues 36−55 in full-length α-Syn (green) bound by an engineered affibody (white) (PDB 4BXL).[19] (B) Chemical structure of the β-hairpin formed by α-Syn$_{36-55}$. (C) Chemical structure of peptide **1a**.

macrocycle to maintain the same alignment and hydrogen-bonding patterns observed in the NMR structure. We replaced the residues that form the loop of the β-hairpin (43−48) with a δ-linked ornithine turn unit, which serves as a β-turn mimic and enforces a β-sheet conformation.[29] We connected residues 36 and 55 with a second δ-linked ornithine turn to further enforce a β-sheet conformation. We mutated Gly$_{36}$ to Ala to enhance the folding of peptide **1a**. We incorporated a single *N*-methyl group on Val$_{52}$ to limit the uncontrolled aggregation of peptide **1a**.[30] We mutated Tyr$_{39}$ to 4-iodophenylalanine (Phe^{I}) to allow X-ray crystallographic phase determination using single wavelength anomalous dispersion (SAD) phasing.

This approach has allowed us to determine the X-ray crystallographic structure of oligomers formed by this β-hairpin derived from α-Syn$_{36-55}$.[31] In this structure, we observe a hierarchical assembly of β-hairpins: three β-hairpins assemble to form a trimer, three trimers assemble to form a nonamer, and two nonamers pack to form an octadecamer. This structure is the first reported X-ray crystallographic structure of oligomeric assemblies of peptides derived from α-Syn. These oligomers suggest a model for α-Syn oligomerization in which self-assembly of α-Syn is centered around α-Syn$_{36-55}$.

RESULTS

X-ray Crystallographic Structure of a Peptide Derived from α-Syn$_{36-55}$. Peptide **1a** and its derivatives were synthesized using Fmoc-based solid-phase peptide synthesis (Scheme S1).[12,30] Screening peptide **1a** in 288 conditions yielded a single condition in which crystals grew: 0.1 M HEPES buffer at pH 8.0, 0.5 M $(NH_4)_2SO_4$, and 34% 2-methyl-2,4-pentanediol (MPD). Diffraction data were collected to 1.97 Å at the Advanced Light Source at Lawrence Berkeley National Laboratory with a synchrotron source at 0.976 Å. Data were scaled and merged with XDS.[32] The locations of the anomalous scattering atoms were determined using the program HySS (hybrid structure search).[33] The structure of peptide **1a** was solved and refined in space group $P2_13$. Coordinates for hydrogen atoms were added during refinement in phenix.refine.[33]

The asymmetric unit contains six distinct copies of peptide **1a**, each of which is folded into an antiparallel β-hairpin with minor differences in the conformations of Thr$_{54}$, Val$_{55}$, and the δ-linked ornithine turn unit that joins Ala$_{36}$ to Val$_{55}$ (Figures 2, S1, and S2). The residues of the β-hairpin are displayed on the front or back surfaces of the β-sheet: Ala$_{36}$, Leu$_{38}$, Val$_{40}$, Ser$_{42}$, Val$_{49}$, Gly$_{51}$, Ala$_{53}$, and Val$_{55}$ are displayed on the front surface; Val$_{37}$, Phe$^{I}_{39}$, Gly$_{41}$, His$_{50}$, *N*-Me Val$_{52}$, and Thr$_{54}$ are displayed on the back surface.[34] The β-hairpin monomers have a right-handed twist ranging from approximately 15−30° per residue along the β-strand axis, thus mimicking the highly twisted β-hairpin observed by Hoyer et al. (Figure 2B).

The differences in conformations of Thr$_{54}$ appear to be responsible for the slight differences among the β-hairpin monomers. Four of the six monomers in the asymmetric unit form an ideal β-hairpin. In the fifth monomer, the hydroxy group of Thr$_{54}$ is positioned such that it disrupts the interchain hydrogen bond between the amide proton of Val$_{55}$ and the

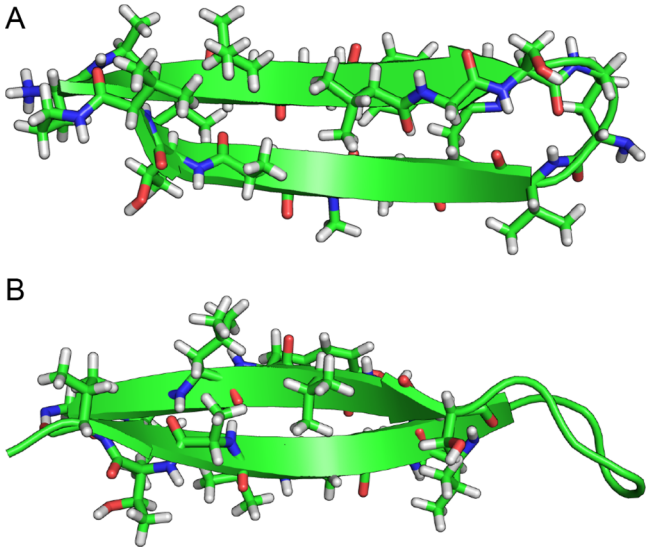

Figure 2. Peptide **1a** mimics the structure of α-Syn$_{36-55}$. (A) Representative β-hairpin monomer from the crystal lattice of peptide **1a** (PDB 5F1T). (B) β-Hairpin monomer formed by α-Syn$_{36-55}$ (PDB 4BXL, affibody omitted).[19]

DOI: 10.1021/jacs.5b13261
J. Am. Chem. Soc. 2016, 138, 4458−4467

carbonyl oxygen of Ala_{36} (Figure S2B). In the sixth monomer, Thr_{54} participates in a γ-turn between Ala_{53} and Val_{55} (Figure S2C). Both of these conformations abrogate the intramolecular hydrogen bonding between Ala_{36} and Val_{55} and distort the conformation of the δ-linked ornithine turn that connects them.

The six β-hairpin monomers of the asymmetric unit further assemble into two triangular trimers in which three monomers occupy the edges of the triangle (Figure 3A). The two trimers differ little in structure. Each trimer is composed of two monomers in one orientation and one monomer in a different orientation. The relative orientations of the *N*-methyl groups within the trimer highlight the lack of internal symmetry; two of the *N*-methyl groups point into the center of the trimer, whereas the third points outward (Figure 3B).

The packing of the monomers in this fashion buries ca. 1300 $Å^2$ of surface area per trimer, averaging 450 $Å^2$ of buried surface area per β-hairpin monomer (Figure 3C). This area corresponds to more than one-fourth of the total surface area of the monomers. The two surfaces of each trimer display different residues: the front surface of each trimer displays the residues on the front surface of the β-hairpin monomers; the back surface of each trimer displays the residues on the back surface β-hairpin monomers. Intermolecular hydrogen bonds at the vertices of the trimer further stabilize this assembly.

The two crystallographically distinct trimers further assemble to form two distinct basket-shaped nonamers, each of which is a trimer of the triangular trimers. (Figure 4A). The two nonamers differ little in structure. Unlike the trimer subunit, each nonamer contains internal *C*3 symmetry, resulting in uniform packing of the trimer subunits against one another. Hydrogen bonding between the trimer subunits stabilizes the basket-shaped nonamer (Figure 4B). The vertices of the trimer subunits within the nonamers form extensive networks of hydrogen bonds. At the juncture of each of the trimers, four β-hairpins come together to form an eight-stranded β-barrel (Figure S3). Each nonamer contains three such β-barrels. The top of the basket-shaped nonamer comprises a hydrogen-bonded triangular interface (Figure 4B). In this interface, each triangular trimer subunit contributes one β-hairpin and each of these β-hairpins forms six intermolecular hydrogen bonds.

Hydrophobic contacts between the triangular trimers also stabilize each nonamer (Figure 4C). The trimer subunits pack against each other along their back surfaces to form a densely packed hydrophobic core consisting of residues Val_{37}, Phe^{I}_{39}, His_{50}, Val_{52}, and Thr_{54}. The front surfaces of the trimer subunits are largely exposed to solvent. The packing of the trimers against one another buries ca. 3000 $Å^2$ of surface area in the nonamer assembly: nearly 1000 $Å^2$ per trimer subunit. This area corresponds to roughly one-third of the total surface area of the trimer.

The two nonamers further dimerize to form an octadecamer (Figure 5A). The nonamers pack against one another through hydrophobic contacts between Ala_{36}, Leu_{38}, Val_{40}, Val_{55}, and the δ-linked ornithine turn unit that connects Ala_{36} to Val_{55} (Figure 5B). This interface buries ca. 1300 $Å^2$ of surface area, of which each nonamer contributes roughly 650 $Å^2$. The octadecamer appears to be the largest oligomer in the crystal lattice. Contacts between octadecamers within the lattice are small, roughly 300 $Å^2$ per octadecamer.

Inspired by the interest in racemic and enantiomeric proteins, we also determined the X-ray crystallographic structure of peptide *ent*-**1a**.[35,36] As expected, peptide *ent*-**1a** crystallizes from the same conditions as peptide **1a** and forms crystals in the same

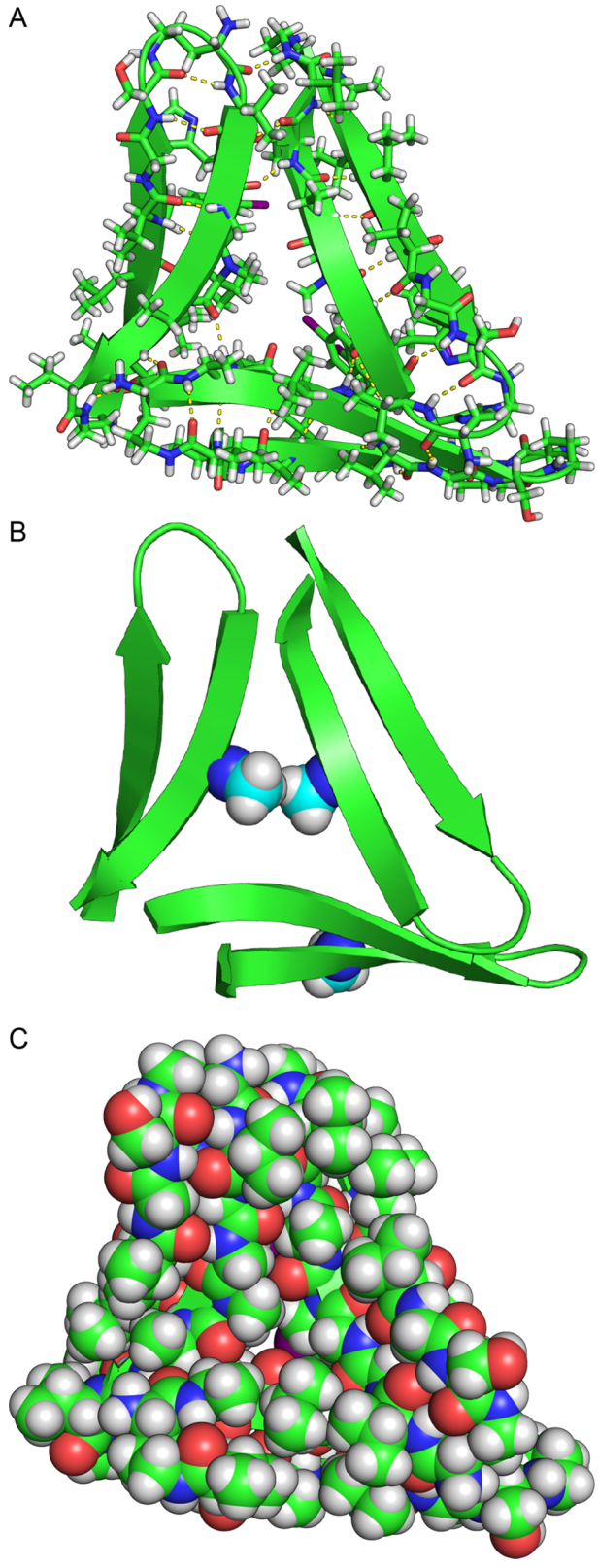

Figure 3. Triangular trimer of peptide **1a**. (A) Cartoon and stick representation depicting the intramolecular and intermolecular hydrogen bonding within the trimer (front surface view). (B) Cartoon representation depicting the location of the *N*-methyl groups in the trimer (front surface view). (C) Sphere representation depicting the hydrophobic packing of residues in the trimer (front surface view).

DOI: 10.1021/jacs.5b13261
J. Am. Chem. Soc. 2016, 138, 4458−4467

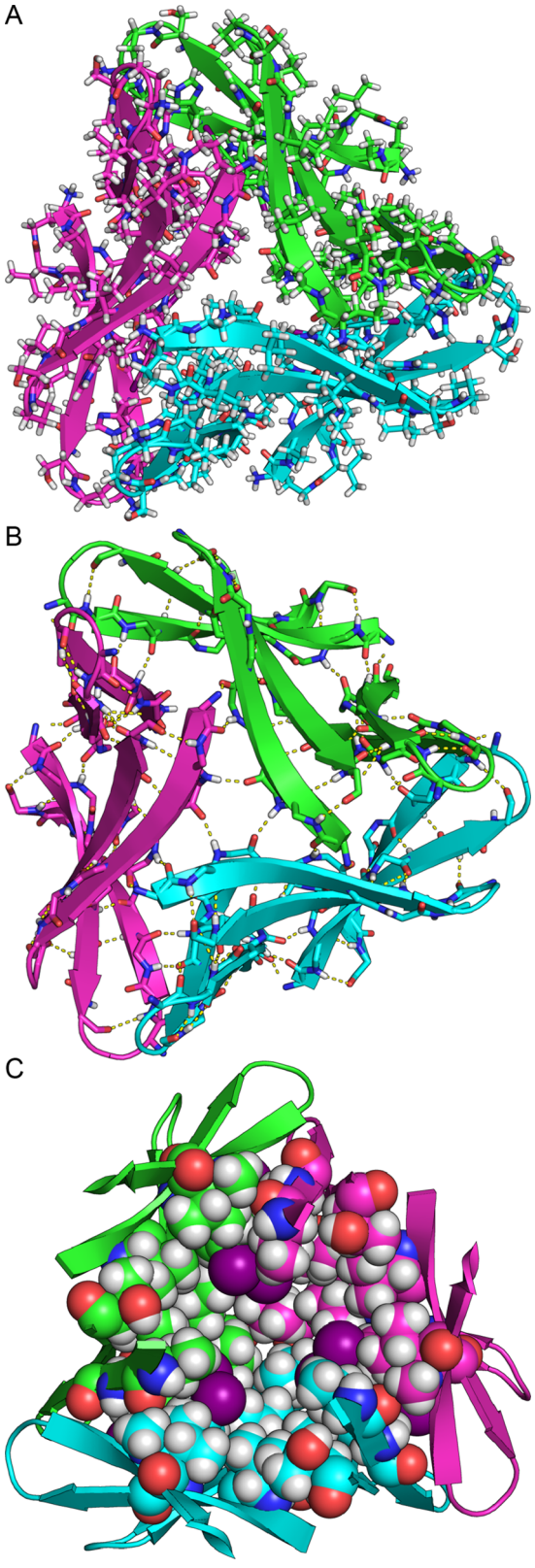

Figure 4. Basket-shaped nonamer formed by peptide **1a**. (A) Cartoon and stick representation (outer surface view). (B) Cartoon and stick representation depicting the main-chain hydrogen-bonding networks (outer surface view). (C) Hydrophobic packing in the core of the nonamer (inner surface view, image is rotated 180° with respect to A and B about the vertical axis).

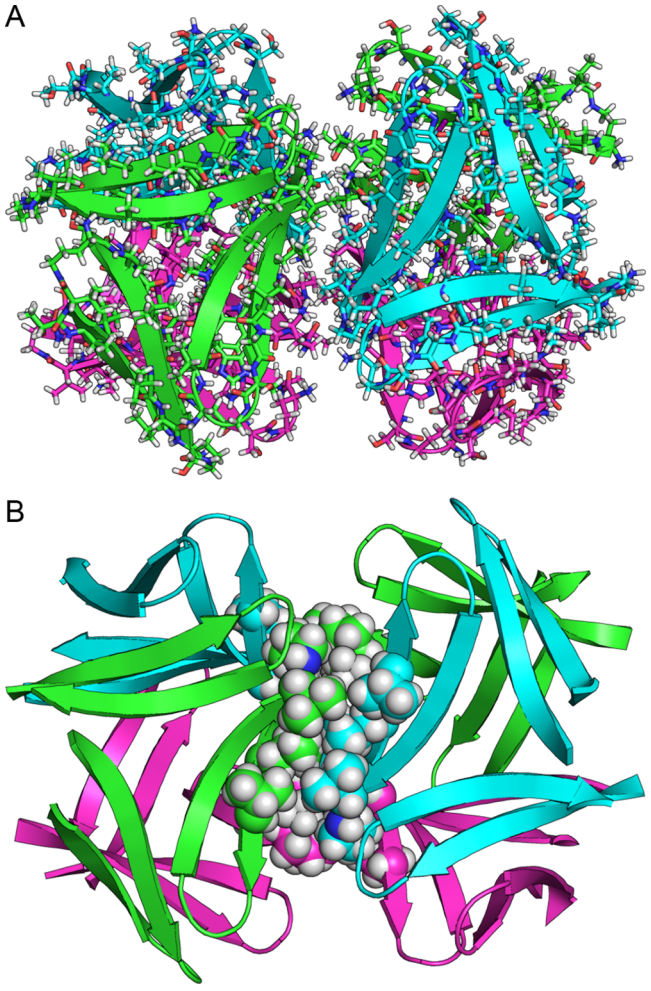

Figure 5. Octadecamer formed by peptide **1a**. (A) Cartoon and stick representation. (B) Sphere representation depicting the contact surface between the nonamer subunits.

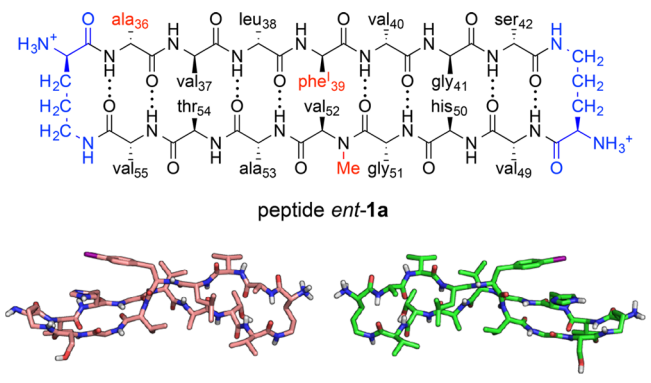

Figure 6. Monomers from the crystal lattice of peptide *ent*-**1a** (left, PDB 5F1W) and peptide **1a** (right, PDB 5F1T). Nonpolar hydrogens are omitted for clarity.

space group with similar unit cell dimensions as those formed by peptide **1a**. The asymmetric unit of peptide *ent*-**1a** contains six molecules of *ent*-**1a**, each of which is folded into a β-hairpin that is the mirror image of that formed by peptide **1a** (Figure 6). Peptide *ent*-**1a** assembles to form oligomers that are mirror images of those formed by peptide **1a**. These enantiomeric oligomers are identical in every fashion, except handedness, to those formed by peptide **1a**. Although racemates often crystallize

DOI: 10.1021/jacs.5b13261
J. Am. Chem. Soc. 2016, 138, 4458−4467

more readily than individual enantiomers, attempts to cocrystallize peptides **1a** and *ent*-**1a** have failed.[37]

Crystallographically Based Model of an α-Syn$_{33-58}$ Nonamer. We envisioned that full-length α-Syn could assemble in the same fashion as the oligomers formed by peptide **1a**, but were concerned whether the trimers and nonamers would accommodate the loop and additional *N*- and *C*-terminal residues. To address this question, we modeled Ac-α-Syn$_{33-58}$-NHMe into the crystallographic coordinates of the nonamer.[38] We built residues 43−48 (KTKEGV), 33−35 (TKE), and 56−58 (AEK) into the crystallographic coordinates of peptide **1a** and performed replica-exchange molecular dynamics (REMD) to generate realistic conformations of the loops and the *N*- and *C*-terminal fragments of the β-hairpin.[39,40] The REMD simulation shows that the nonamer successfully accommodates the additional residues from the full-length protein without any significant clashes among residues (Figure 7). The N- and C-terminal fragments of α-Syn project out of the assembly and do not interfere with nonamer formation. The residues on each of the loops at the vertices of the nonamer pack against one another, suggesting that these additional residues from the full-length protein could stabilize this assembly. Incorporation of the loops as well as the additional N- and C-terminal residues into the nonamer buries an additional 400 Å^2 of surface area per trimer subunit, providing an additional 1200 Å^2 of buried surface area beyond the crystallographic nonamer. Table 1 summarizes the size of the contact surfaces within the crystallographic oligomers and the model of α-Syn$_{33-58}$. The X-ray crystallographic and REMD structures generated herein may serve as models for the core of the oligomers formed by full-length α-Syn.

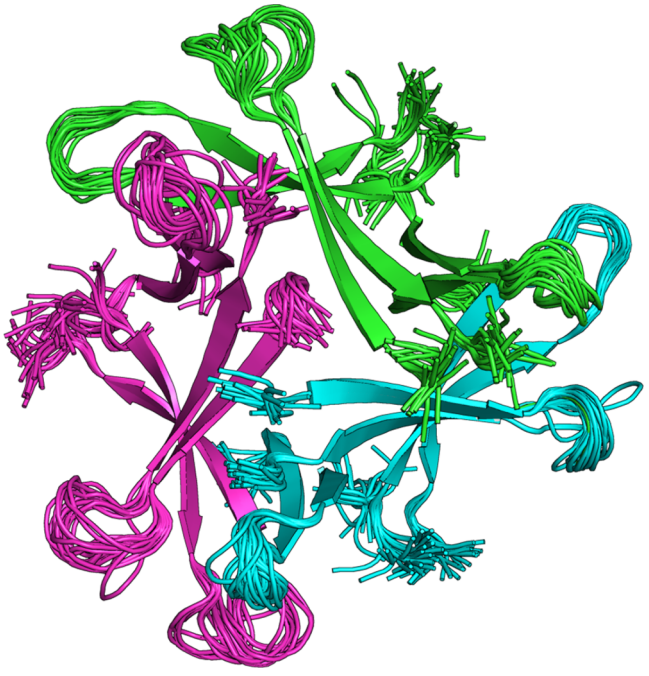

Figure 7. Crystallographically based model of the α-Syn$_{33-58}$ nonamer. Superposition of 20 structures of Ac-α-Syn$_{33-58}$-NHMe generated by replica-exchange molecular dynamics.

Table 1. Buried Surface Area within the Oligomers Formed by Peptides 1a and the α-Syn$_{33-58}$ Model

assembly	subunit	BSA (Å^2)[a]	BSA/subunit (Å^2)[b]
trimer (**1a**)	monomer	1300	450
trimer (model)	monomer	1700	550
nonamer (**1a**)	trimer	3000	1000
nonamer (model)	trimer	4200	1400

[a]Buried surface area. [b]Average BSA per subunit.

Membrane-Induced Folding of Peptides Derived from α-Syn$_{36-55}$. The interaction of α-Syn with the anionic membranes of neurons induces conformational changes and nucleates self-assembly of the protein.[41] To test the effects of membranes on the conformation of peptide **1a**, we compared the circular dichroism (CD) spectra of peptide **1a** in the presence of anionic or neutral liposomes to that of peptide **1a** in aqueous buffer (Figure 8).[42−44] The CD spectrum of peptide **1a** in aqueous buffer displays negative bands centered at 220 and 200 nm.[45] Upon the addition of anionic phosphatidylcholine:phosphatidylserine (PC:PS) large unilamellar vesicles (LUVs), the CD spectrum of peptide **1a** changes dramatically: the negative band at 220 nm becomes more intense and a positive band appears below ca. 210 nm. This change in CD spectrum upon addition of the liposomes indicates that peptide **1a** adopts a β-sheet-rich conformation upon interaction with anionic PC:PS liposomes.

In contrast to anionic PC:PS LUVs, neutral phosphatidylcholine (PC) LUVs do not induce changes in the conformation of peptide **1a**. The CD spectrum of peptide **1a** in the presence of PC LUVs is superimposable with the CD spectrum of peptide **1a** in aqueous buffer. The contrasting effects of the PC and PC:PS

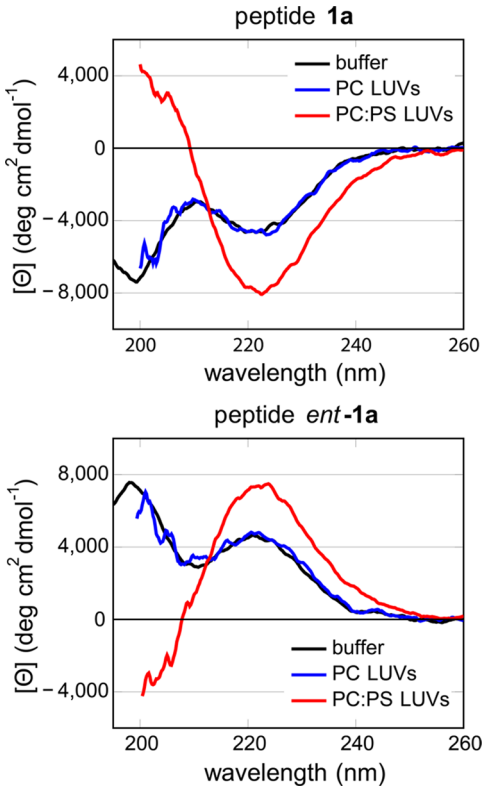

Figure 8. Effects of liposomes on the CD spectra of peptide **1a** and *ent*-**1a**. Spectra of 50 μM peptide in 10 mM sodium phosphate buffer at pH 7.4 were acquired in the presence or absence of 1.0 mM lipids, constituting either phosphatidylcholine (PC) or phosphatidylcholine:-phosphatidylserine (PC:PS) liposomes. Data are graphed as mean residue ellipticity. The CD spectra could not be recorded below ca. 200 nm in the presence of the liposomes.

DOI: 10.1021/jacs.5b13261
J. Am. Chem. Soc. 2016, 138, 4458−4467

liposomes indicates that electrostatic interactions between the cationic peptide and the anionic liposomes are essential to the membrane-induced conformational changes observed.

To test the importance of chirality in the interaction of peptide **1a** with PC:PS liposomes, we investigated the effect of liposomes on the CD spectra of peptide *ent*-**1a**. The CD spectra of peptide *ent*-**1a** are identical but opposite in sign to those of peptide **1a** in the three sets of conditions studied. In aqueous buffer, the CD spectrum of peptide *ent*-**1a** displays positive bands centered at 220 and 200 nm. In the presence of PC:PS LUVs, the positive band at 220 nm becomes more intense and a negative band appears below ca. 210 nm. No change in the CD spectrum is observed upon the addition of PC LUVs. The equivalent behavior of the enantiomeric peptide suggests that chiral interactions are not important in the interaction with liposomes, even though the individual lipid molecules are chiral. Instead, the interaction appears to reflect the importance of the charged head groups and the hydrophobic lipids.

Cytotoxicity of Peptides Derived from α-Syn$_{36-55}$. The oligomers formed by full-length α-Syn are thought to induce cell death upon interaction with the cell membrane.[46] To determine whether the propensity of peptide **1a** to bind lipid membranes imparts toxicity, we studied the effect of peptide **1a** and several control peptides on a neuronally derived cell line. Treatment of SH-SY5Y cells with peptide **1a** results in cell death as measured by lactate dehydrogenase release (LDH) and 3-(4,5-dimethylthiazol-2-yl)-2,5-diphenyltetrazolium bromide (MTT) conversion assays (Figure 9). A dose-response relationship is observed at concentrations ranging from 5−40 μM, with maximal toxicity occurring at 40 μM. Maximal cell death occurs within 16 h after treatment with 40 μM peptide **1a** (Figure S4). These results demonstrate that peptide **1a** is cytotoxic but do not establish that the toxicity results from membrane interaction.

To establish whether cell death occurs from membrane interaction, we compared peptide **1a** to three homologues (*ent*-**1a**, **1a**$_{A53E}$, and **1b**) in LDH and MTT assays (Figure 10). Treatment of SH-SY5Y cells with either peptide *ent*-**1a** or peptide **1a** results in nearly equal levels of cell death. The comparable toxicity of peptides *ent*-**1a** and **1a** suggest that toxicity results from nonspecific interactions with the cells, rather than through specific interaction with a receptor protein.

Peptide **1a**$_{A53E}$ is identical to peptide **1a** in amino acid sequence with exception of the A53E familial point mutation. This mutation reduces the affinity of full-length α-Syn to anionic lipid membranes and delays its aggregation.[27] CD spectroscopy shows that this mutation blocks interactions between peptide **1a**$_{A53E}$ and anionic lipid membranes: the CD spectra of peptide **1a**$_{A53E}$ are identical in the presence or absence of PC:PS LUVs (Figure S5). Peptide **1a**$_{A53E}$ produces no measurable cell death at 40 uM (Figure 10). The lack of toxicity of peptide **1a**$_{A53E}$ in conjunction with its lack of membrane interactions supports that membrane interaction is central to the toxicity of peptide **1a**.

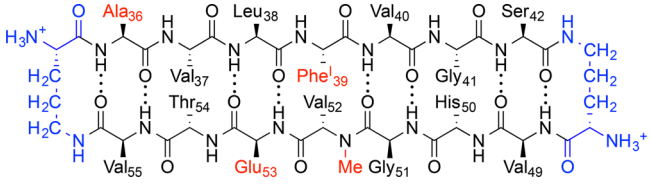

peptide **1a**$_{A53E}$

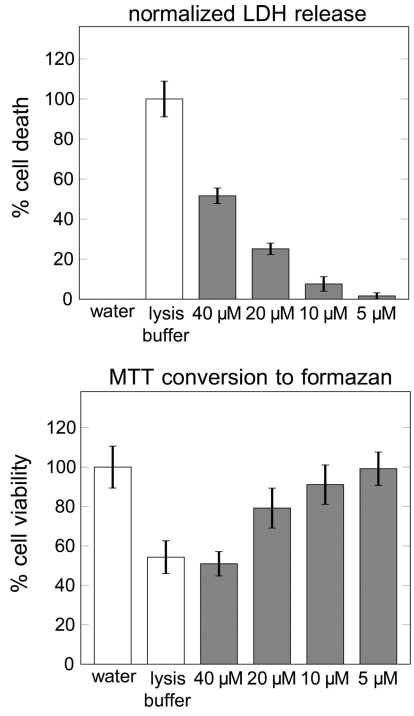

Figure 9. LDH and MTT assays of the toxicity of peptide **1a** toward SH-SY5Y cells. Cells were incubated with 5−40 μM of peptide **1a** for 24 h before performing the assays. Cell death and viability were determined spectrophotometrically as previously described.[47,48] Error bars represent standard deviation propagated from five replicate runs.

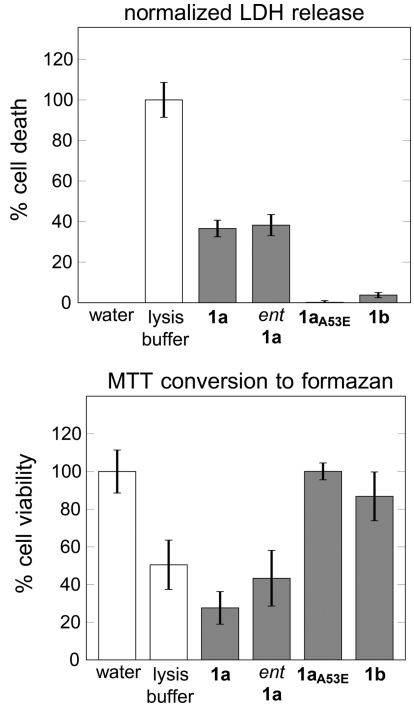

Figure 10. LDH and MTT assays of the toxicity of peptide **1a** and its homologues toward SH-SY5Y cells. Cells were incubated with 40 μM of peptide **1a**, *ent*-**1a**, **1a**$_{A53E}$, or **1b** for 24 h before performing the assays. Cell death and viability were determined spectrophotometrically as previously described.[47,48] Error bars represent standard deviation propagated from five replicate runs.

DOI: 10.1021/jacs.5b13261
J. Am. Chem. Soc. 2016, 138, 4458−4467

Peptide **1b** was designed to test the role of the crystallographically observed oligomers in the toxicity elicited by peptide **1a**. Peptide **1b** is identical to peptide **1a** in amino acid sequence, but is *N*-methylated at Gly_{41} instead of Val_{52}. We anticipated that *N*-methylation at Gly_{41} would disrupt the formation of the trimer and the basket-shaped nonamer by disrupting the hydrogen-bonding within the oligomers and forcing the subunits apart (Figure S6). Peptide **1b** is much less cytotoxic than peptide **1a**, as determined by both the LDH and MTT assays (Figure 10). *N*-Methylation at Gly_{41} does not impair the interaction of peptide **1b** and lipid bilayer membranes: upon the addition of PC:PS LUVs, the CD spectrum of peptide **1b** changes dramatically, in a fashion similar to the changes observed for peptide **1a** (Figure S5). The marked decrease in toxicity of peptide **1b** is consistent with, but does not prove, the involvement of the crystallographically observed oligomers in the cytotoxicity associated with peptide **1a**.

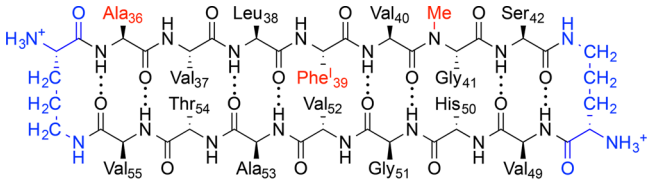

peptide **1b**

DISCUSSION

The X-ray crystallographic studies of peptide **1a** and the molecular modeling studies of the α-Syn_{33-58} nonamer suggest a model for oligomer formation by full-length α-Syn. In this model, residues 36−55 of full-length α-Syn form a β-hairpin, three of these β-hairpins assemble to form triangular trimers, and the trimers assemble to form basket-shaped nonamers or related higher-order oligomers. To our knowledge, the X-ray crystallographic structure of peptide **1a** provides the first high-resolution structures of oligomers of peptides derived from α-Syn. There are currently no reported high-resolution structures of oligomers of the full-length protein. The structures described herein should help bridge the gap between the plethora of low-resolution structural information on full-length α-Syn oligomers and a still needed high-resolution structure.

The structures of the oligomers formed by peptide **1a** are fundamentally different from the proposed structure of the fibrils formed by α-Syn (Figure 11).[49,50] Although there are no high-resolution structures of the fibrils formed by full-length α-Syn, the current understanding of fibril structures suggests that the monomer units fold onto themselves to form a five-layer β-sandwich. In the fibril, the folded monomers hydrogen bond with neighboring monomers to form a network of parallel β-sheets. Although many of the details of the fibril assembly are still being debated, commonalities such as multilayered parallel β-sheets are widely accepted.[51−57] In contrast to the proposed assembly of the fibril, the oligomers we observe assemble in a different fashion: through the intermolecular interactions among antiparallel β-hairpins. This difference may suggest that the oligomers formed by full-length α-Syn differ from the fibrils in both monomer conformation and in themes of higher-order assembly.

The X-ray crystallographic structure of peptide **1a** suggests an alternative model for oligomer formation by full-length α-Syn centered around residues 36−55, rather than the NAC (Figure 11). Residues 61−95 of α-Syn, termed the NAC,[58] are required

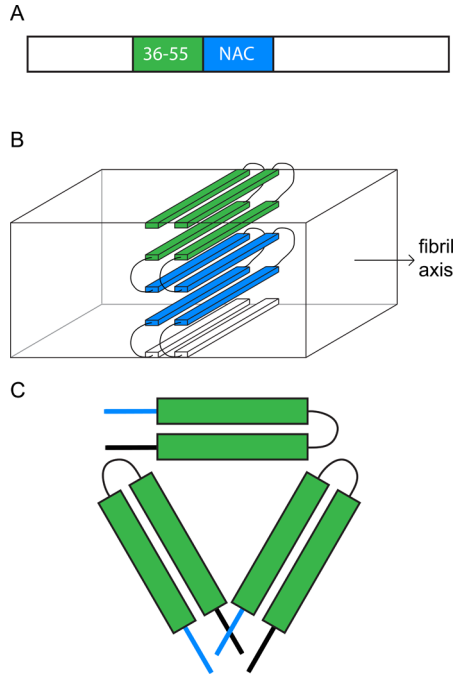

Figure 11. Models of an α-Syn fibril and an α-Syn oligomer. (A) Cartoon of α-Syn monomer. Residues 36−55 are colored green and the NAC is colored blue. (B) Cartoon of α-Syn fibril, showing two monomer subunits arranged into a five-layered β-sheet.[50] (C) Cartoon of α-Syn trimer subunit of basket-shaped nonamers or related higher-order oligomers, showing three β-hairpins arranged into a trimer.

for fibrillization of the protein.[59−62] The currently accepted model of the α-Syn fibril places the NAC at the core of the assembly and α-Syn_{36-55} at the periphery.[63] The alternative oligomer model places α-Syn_{36-55} at the core of the oligomers, while the NAC and remainder of the protein decorates the periphery. This model does not rule out the possibility of other types of α-Syn oligomers with the NAC at their core. As α-Syn oligomers are known to be polymorphic, there may be multiple families of oligomers in which different regions of α-Syn drive assembly.

The occurrence of five of the six known familial point mutations in α-Syn_{36-55} suggests that this region is important in the pathology of synucleinopathies. With exception of H50Q, all of these point mutations would be displayed on the solvent-exposed surface of the basket-shaped nonamer. These mutations might stabilize the nonamers or component trimers, or might drive the protein into oligomers with different structures. Alternatively, these mutations may merely destabilize native tetramers of α-Syn and thus promote aggregation.[64,65] An X-ray crystallographic structure of a derivative of peptide **1a** bearing any of these point mutations would be edifying. Our own attempts to crystallize homologues of peptide **1a** with point mutations H50Q, G51D, A53E, or A53T have thus far been unsuccessful.

The oligomers formed by full-length α-Syn may differ from those formed by peptide **1a** while still retaining the general features of β-hairpins and trimers. We have, for example, observed that β-hairpins derived from β-amyloid and β_2-microglobulin form symmetrical trimers, rather than the asymmetric trimer observed for peptide **1a**.[12,13] These trimers further assemble to form hexamers, octamers, and dodecamers instead of nonamers and octadecamers. Although all of these amyloid-derived peptides differ in sequence and the oligomers

DOI: 10.1021/jacs.5b13261
J. Am. Chem. Soc. 2016, 138, 4458−4467

differ in precise structure, they share the common theme of β-hairpins assembling into triangular trimers that further assemble into complex and intricate higher-order assemblies.

Trimers may be a unifying motif of toxic amyloid oligomers formed by full-length amyloidogenic proteins. SDS-stable trimeric assemblies of full-length α-Syn have been observed in immunoblots of mouse brain extracts.[4] The appearance of these species strongly correlates with an increased loss of dopaminergic neurons in vivo. Similarly, trimeric assemblies of β-amyloid have been shown to disrupt cognitive function in rats.[66] The occurrence of the triangular trimeric motif in crystal structures reported by our group has led us to believe that trimers may be unifying substructures of amyloid oligomers that are composed of β-hairpin monomers. The CD studies, in conjunction with the toxicity assays, suggest that the cytotoxicity of peptide **1a** may result from interactions of trimers or higher-order oligomers with cell membranes, in the same fashion as the oligomers of full-length α-Syn.[2] At this point, we cannot conclusively say that the crystallographic oligomers are forming under the conditions used in the cell assays;[67] however, the substantial decrease in toxicity of the alternatively *N*-methylated peptide **1b** supports the involvement of the trimer and/or nonamers in cell death.

CONCLUSION

Here we present the first X-ray crystallographic structure of oligomers formed by a peptide derived from α-Syn. This peptide was designed to mimic a β-hairpin motif thought to be important in α-Syn oligomer formation. This designed peptide mimics key properties of oligomers of full-length α-Syn: affinity for membranes that imparts toxicity. The structure suggests a model for α-Syn oligomer formation centered around α-Syn$_{36-55}$, in which α-Syn$_{36-55}$ folds into a β-hairpin that further assembles into trimers and higher-order oligomers. These structures differ in topology from those of α-Syn fibrils and suggest that regions of α-Syn not important for its fibrillization may play a central role in its oligomerization. The X-ray crystallographic structure of peptide **1a** and the model of the α-Syn$_{33-58}$ nonamer may be used as starting points to design small molecules that interact with α-Syn oligomers or to rationalize the modes of interactions between α-Syn oligomers and small molecules that interact with them.

ASSOCIATED CONTENT

Supporting Information

The Supporting Information is available free of charge on the ACS Publications website at DOI: 10.1021/jacs.5b13261. Crystallographic coordinates of peptides **1a** and *ent*-**1a** were deposited into the Protein Data Bank (PDB) with codes 5F1T and 5F1W.

Procedures for the synthesis and crystallization of peptides **1a**, *ent*-**1a**, **1a**$_{A53E}$, and **1b**; details of X-ray diffraction data collection, processing, and refinement; details for REMD; details for cell culture, MTT, and LDH assays (PDF)

Crystallographic details for **1a** (CIF)

Crystallographic details for *ent*-**1a** (CIF)

Ac-α-Syn$_{33-58}$-NHMe modeled into the basket-shaped nonamer (PDB)

AUTHOR INFORMATION

Corresponding Author

*jsnowick@uci.edu

Notes

The authors declare no competing financial interest.

ACKNOWLEDGMENTS

This work was supported by the National Science Foundation (NSF CHE-1507840). P.J.S. thanks the UCI Training Program in Chemical and Structural Biology for training grant support (T32 GM108561). The Berkeley Center for Structural Biology is supported in part by the National Institutes of Health, National Institute of General Medical Sciences, and the Howard Hughes Medical Institute. The Advanced Light Source is supported by the Director, Office of Science, Office of Basic Energy Sciences, of the U.S. Department of Energy under Contract No. DE-AC02-05CH11231. The authors thank the Laser Spectroscopy Facility at University of California, Irvine for assistance with circular dichroism measurements.

REFERENCES

(1) Breydo, L.; Wu, J. W.; Uversky, V. N. *Biochim. Biophys. Acta, Mol. Basis Dis.* **2012**, *1822*, 261−285.

(2) Lashuel, H. A.; Overk, C. R.; Oueslati, A.; Masliah, E. *Nat. Rev. Neurosci.* **2013**, *14*, 38−48.

(3) Bendor, J. T.; Logan, T. P.; Edwards, R. H. *Neuron* **2013**, *79*, 1044−1066.

(4) Winner, B.; Jappelli, R.; Maji, S. K.; Desplats, P. A.; Boyer, L.; Aigner, S.; Hetzer, C.; Loher, T.; Vilar, M.; Campioni, S.; Tzitzilonis, C.; Soragni, A.; Jessberger, S.; Mira, H.; Consiglio, A.; Pham, E.; Masliah, E.; Gage, F. H.; Riek, R. *Proc. Natl. Acad. Sci. U. S. A.* **2011**, *108*, 4194−4199.

(5) Chen, S. W.; Drakulic, S.; Deas, E.; Ouberai, M.; Aprile, F. A.; Arranz, R.; Ness, S.; Roodveldt, C.; Guilliams, T.; De-Genst, E. J.; Klenerman, D.; Wood, N. W.; Knowles, T. P. J.; Alfonso, C.; Rivas, G.; Abramov, A. Y.; Valpuesta, J. M.; Dobson, C. M.; Cremades, N. *Proc. Natl. Acad. Sci. U. S. A.* **2015**, *112*, E1994−E2003.

(6) Liu, C.; Sawaya, M. R.; Cheng, P.-N.; Zheng, J.; Nowick, J. S.; Eisenberg, D. *J. Am. Chem. Soc.* **2011**, *133*, 6736−6744.

(7) Laganowsky, A.; Liu, C.; Sawaya, M. R.; Whitelegge, J. P.; Park, J.; Zhao, M.; Pensalfini, A.; Soriaga, A. B.; Landau, M.; Teng, P. K.; Cascio, D.; Glabe, C.; Eisenberg, D. *Science* **2012**, *335*, 1228−1231.

(8) Apostol, M. I.; Perry, K.; Surewicz, W. K. *J. Am. Chem. Soc.* **2013**, *135*, 10202−10205.

(9) Pham, J. D.; Chim, N.; Goulding, C. W.; Nowick, J. S. *J. Am. Chem. Soc.* **2013**, *135*, 12460−12467.

(10) Pham, J. D.; Demeler, B.; Nowick, J. S. *J. Am. Chem. Soc.* **2014**, *136*, 5432−5442.

(11) Pham, J. D.; Spencer, R. K.; Chen, K. H.; Nowick, J. S. *J. Am. Chem. Soc.* **2014**, *136*, 12682−12690.

(12) Spencer, R. K.; Li, H.; Nowick, J. S. *J. Am. Chem. Soc.* **2014**, *136*, 5595−5598.

(13) Spencer, R. K.; Kreutzer, A. G.; Salveson, P. J.; Li, H.; Nowick, J. S. *J. Am. Chem. Soc.* **2015**, *137*, 6304−6311.

(14) Teoh, C. L.; Su, D.; Sahu, S.; Yun, S.-W.; Drummond, E.; Prelli, F.; Lim, S.; Cho, S.; Ham, S.; Wisniewski, T.; Chang, Y.-T. *J. Am. Chem. Soc.* **2015**, *137*, 13503−13509.

(15) Do, T. D.; LaPointe, N. E.; Nelson, R.; Krotee, P.; Hayden, E. Y.; Ulrich, B.; Quan, S.; Feinstein, S. C.; Teplow, D. B.; Eisenberg, D.; Shea, J.-E.; Bowers, M. T. *J. Am. Chem. Soc.* **2016**, *138*, 549−557.

(16) Celej, M. S.; Sarroukh, R.; Goormaghtigh, E.; Fidelio, G. D.; Ruysschaert, J.-M.; Raussens, V. *Biochem. J.* **2012**, *443*, 719−726.

(17) Gallea, J. I.; Celej, M. S. *J. Biol. Chem.* **2014**, *289*, 26733−26742.

(18) Paslawski, W.; Mysling, S.; Thomsen, K.; Jørgensen, T. J. D.; Otzen, D. E. *Angew. Chem., Int. Ed.* **2014**, *53*, 7560−7563.

(19) Mirecka, E. A.; Shaykhalishahi, H.; Gauhar, A.; Akgül, S.; Lecher, J.; Willbold, D.; Stoldt, M.; Hoyer, W. *Angew. Chem., Int. Ed.* **2014**, *53*, 4227−4230.

(20) Dedmon, M. M.; Lindorff-Larsen, K.; Christodoulou, J.; Vendruscolo, M.; Dobson, C. M. *J. Am. Chem. Soc.* **2005**, *127*, 476−477.

DOI: 10.1021/jacs.5b13261
J. Am. Chem. Soc. 2016, 138, 4458−4467

(21) Esteban-Martín, S.; Silvestre-Ryan, J.; Bertoncini, C. W.; Salvatella, X. *Biophys. J.* **2013**, *105*, 1192−1198.
(22) Polymeropoulos, M. H.; Lavedan, C.; Leroy, E.; Ide, S. E.; Dehejia, A.; Dutra, A.; Pike, B.; Root, H.; Rubenstein, J.; Boyer, R.; Stenroos, E. S.; Chandrasekharappa, S.; Athanassiadou, A.; Papapetropoulos, T.; Johnson, W. G.; Lazzarini, A. M.; Duvoisin, R. C.; Di Iorio, G.; Globe, L. I.; Nussbaum, R. L. *Science* **1997**, *276*, 2045−2047.
(23) Krüger, R.; Kuhn, W.; Müller, T.; Woitalla, D.; Graeber, M.; Kösel, S.; Przuntek, H.; Epplen, J. T.; Schols, L.; Riess, O. *Nat. Genet.* **1998**, *18*, 106−108.
(24) Zarranz, J. J.; Alegre, J.; Gómez-Esteban, J. C.; Lezcano, E.; Ros, R.; Ampuero, I.; Vidal, L.; Hoenicka, J.; Rodriguez, O.; Atarés, B.; Llorens, V.; Tortosa, E. G.; del Ser, T.; Muñoz, D. G.; de Yebenes, J. G. *Ann. Neurol.* **2004**, *55*, 164−173.
(25) Appel-Cresswell, S.; Vilarino-Guell, C.; Encarnacion, M.; Sherman, H.; Yu, I.; Shah, B.; Weir, D.; Thompson, C.; Szu-tu, C.; Trinh, J.; Aasly, J. O.; Rajput, A.; Rajput, A. H.; Stoessl, A. J.; Farrer, M. J. *Mov. Disord.* **2013**, *28*, 811−813.
(26) Lesage, S.; Anheim, M.; Letournel, F.; Bousset, L.; Honoré, A.; Rozas, N.; Pieri, L.; Madiona, K.; Dürr, A.; Melki, R.; Verny, C.; Brice, A. *Ann. Neurol.* **2013**, *73*, 459−471.
(27) Ghosh, D.; Sahay, S.; Ranjan, P.; Salot, S.; Mohite, G. M.; Singh, P. K.; Dwivedi, S.; Carvalho, E.; Banerjee, R.; Kumar, A.; Maji, S. K. *Biochemistry* **2014**, *53*, 6419−6421.
(28) Yu, H.; Han, W.; Ma, W.; Schulten, K. *J. Chem. Phys.* **2015**, *143*, 243142.
(29) Nowick, J. S.; Brower, J. O. *J. Am. Chem. Soc.* **2003**, *125*, 876−877.
(30) Spencer, R. K.; Chen, K. H.; Manuel, G.; Nowick, J. S. *Eur. J. Org. Chem.* **2013**, *2013*, 3523−3528.
(31) Spencer, R. K.; Nowick, J. S. *Isr. J. Chem.* **2015**, *55*, 698−710.
(32) Kabsch, W. *Acta Crystallogr., Sect. D: Biol. Crystallogr.* **2010**, *66*, 125−132.
(33) Adams, P. D.; Afonine, P. V.; Bunkóczi, G.; Chen, V. B.; Davis, I. W.; Echols, N.; Headd, J. J.; Hung, L.-W.; Kapral, G. J.; Grosse-Kunstleve, R. W.; McCoy, A. J.; Moriarty, N. W.; Oeffner, R.; Read, R. J.; Richardson, D. C.; Richardson, J. S.; Terwilliger, T. C.; Zwart, P. H. *Acta Crystallogr., Sect. D: Biol. Crystallogr.* **2010**, *66*, 213−221.
(34) Cheng, P.-N.; Pham, J. D.; Nowick, J. S. *J. Am. Chem. Soc.* **2013**, *135*, 5477−5492.
(35) Milton, R. C.; Milton, S. C.; Kent, S. B. *Science* **1992**, *256*, 1445−1448.
(36) Yeates, T. O.; Kent, S. B. *Annu. Rev. Biophys.* **2012**, *41*, 41−61.
(37) For examples of racemic peptide crystallography, see: (a) Mortenson, D. E.; Satyshur, K. A.; Guzei, I. A.; Forest, K. T.; Gellman, S. H. *J. Am. Chem. Soc.* **2012**, *134*, 2473−2476. (b) Wang, C. K.; King, G. J.; Northfield, S. E.; Ojeda, P. G.; Craik, D. *Angew. Chem., Int. Ed.* **2014**, *53*, 11236−11241. (c) Hayouka, Z.; Thomas, N. C.; Mortenson, D. E.; Satyshur, K. A.; Weisblum, B.; Forest, K. T.; Gellman, S. H. *J. Am. Chem. Soc.* **2015**, *137*, 11884−11887. (d) Mortenson, D. E.; Steinkruger, J. D.; Kreitler, D. F.; Perroni, D. V.; Sorenson, G. P.; Huang, L.; Mittal, R.; Yun, H. G.; Travis, B. R.; Mahanthappa, M. K.; Forest, K. T.; Gellman, S. H. *Proc. Natl. Acad. Sci. U. S. A.* **2015**, *112*, 13144−13149.
(38) For an excellent review using simulation-based approaches to understand the structures of oligomers formed by the β-amyloid peptide, see: Nasica-Labouze, J.; Nguyen, P. H.; Sterpone, F.; Berthoumieu, O.; Buchete, N.-V.; Cote, S.; De Simone, A.; Doig, A. J.; Faller, P.; Garcia, A.; Laio, A.; Li, M. S.; Melchionna, S.; Mousseau, N.; Mu, Y.; Paravastu, A.; Pasquali, S.; Rosenman, D. J.; Strodel, B.; Tarus, B.; Viles, J. H.; Zhang, T.; Wang, C.; Derreumaux, P. *Chem. Rev.* **2015**, *115*, 3518−3563.
(39) Sugita, Y.; Okamoto, Y. *Chem. Phys. Lett.* **1999**, *314*, 141−151.
(40) Phillips, J. C.; Braun, R.; Wang, W.; Gumbart, J.; Tajkhorshid, E.; Villa, E.; Chipot, C.; Skeel, R. D.; Kalé, L.; Schulten, K. *J. Comput. Chem.* **2005**, *26*, 1781−1802.
(41) Galvagnion, C.; Buell, A. K.; Meisl, G.; Michaels, T. C. T.; Vendruscolo, M.; Knowles, T. P. J.; Dobson, C. M. *Nat. Chem. Biol.* **2015**, *11*, 229−234.
(42) Kelly, S. M.; Jess, T. J.; Price, N. C. *Biochim. Biophys. Acta, Proteins Proteomics* **2005**, *1751*, 119−139.
(43) Greenfield, N. J. *Nat. Protoc.* **2007**, *1*, 2876−2890.
(44) Sinthuvanich, C.; Veiga, A. S.; Gupta, K.; Gaspar, D.; Blumenthal, R.; Schneider, J. P. *J. Am. Chem. Soc.* **2012**, *134*, 6210−6217.
(45) The CD spectra of short peptides folded into well-defined β-hairpins often do not display canonical β-sheet signatures: a negative band at ca. 220 nm and a positive band below 200 nm. To the best of our knowledge, there is no singular CD signature for a β-hairpin, even in cases where a β-hairpin conformation is evident in NMR spectra. For examples of CD spectra of well-defined β-hairpins, see: (a) Blanco, F. J.; Rivas, G.; Serrano, L. *Nat. Struct. Biol.* **1994**, *1*, 584−590. (b) Stanger, H. E.; Gellman, S. H. *J. Am. Chem. Soc.* **1998**, *120*, 4236−4237. (c) Andersen, N. H.; Olsen, K. A.; Fesinmeyer, R. M.; Tan, X.; Hudson, F. M.; Eidenschink, L. A.; Farazi, S. R. *J. Am. Chem. Soc.* **2006**, *128*, 6101−6110. (d) Cline, L. L.; Waters, M. L. *Biopolymers* **2009**, *92*, 502−507. (e) Kier, B. L.; Shu, I.; Eidenschink, L. A.; Andersen, N. H. *Proc. Natl. Acad. Sci. U. S. A.* **2010**, *107*, 10466−10471.
(46) Auluck, P. K.; Caraveo, G.; Lindquist, S. *Annu. Rev. Cell Dev. Biol.* **2010**, *26*, 211−233.
(47) Korzeniewski, C.; Callewaert, D. M. *J. Immunol. Methods* **1983**, *64*, 313−320.
(48) Mosmann, T. *J. Immunol. Methods* **1983**, *65*, 55−63.
(49) Der-Sarkissian, A.; Jao, C. C.; Chen, J.; Langen, R. *J. Biol. Chem.* **2003**, *278*, 37530−37535.
(50) Vilar, M.; Chou, H.-T.; Lührs, T.; Maji, S. K.; Riek-Loher, D.; Verel, R.; Manning, G.; Stahlberg, H.; Riek, R. *Proc. Natl. Acad. Sci. U. S. A.* **2008**, *105*, 8637−8642.
(51) Heise, H.; Hoyer, W.; Becker, S.; Andronesi, O. C.; Riedel, D.; Baldus, M. *Proc. Natl. Acad. Sci. U. S. A.* **2005**, *102*, 15871−15876.
(52) Comellas, G.; Lemkau, L. R.; Nieuwkoop, A. J.; Kloepper, K. D.; Ladror, D. T.; Ebisu, R.; Woods, W. S.; Lipton, A. S.; George, J. M.; Rienstra, C. M. *J. Mol. Biol.* **2011**, *411*, 881−895.
(53) Comellas, G.; Lemkau, L. R.; Zhou, D. H.; George, J. M.; Rienstra, C. M. *J. Am. Chem. Soc.* **2012**, *134*, 5090−5099.
(54) Lv, G.; Kumar, A.; Giller, K.; Orcellet, M. L.; Riedel, D.; Fernández, C. O.; Becker, S.; Lange, A. *J. Mol. Biol.* **2012**, *420*, 99−111.
(55) Gath, J.; Habenstein, B.; Bousset, L.; Melki, R.; Meier, B. H. *Biomol. NMR Assignments* **2012**, *6*, 51−55.
(56) Gath, J.; Bousset, L.; Habenstein, B.; Melki, R.; Meier, B. H.; Böckmann, A. *Biomol. NMR Assignments* **2014**, *8*, 395−404.
(57) Verasdonck, J.; Bousset, L.; Gath, J.; Melki, R.; Böckmann, A.; Meier, B. H. *Biomol. NMR Assignments* **2015**, 1−8.
(58) The term NAC stands for non-β-amyloid component of β-amyloid plaques. The NAC was first identified as a 35-residue peptide that coaggregated with β-amyloid in the brains of Alzheimer's disease patients: Uéda, K.; Fukushima, H.; Masliah, E.; Xia, Y.; Iwai, A.; Yoshimoto; Otero, D. A.; Kondo, J.; Ihara, Y.; Saitoh, T. *Proc. Natl. Acad. Sci. U. S. A.* **1993**, *90*, 11282−11286.
(59) Giasson, B. I.; Murray, I. V. J.; Trojanowski, J. Q.; Lee, V. M.-Y. *J. Biol. Chem.* **2001**, *276*, 2380−2386.
(60) Du, H.-N.; Tang, L.; Luo, X.-Y.; Li, H.-T.; Hu, J.; Zhou, J.-W.; Hu, H.-Y. *Biochemistry* **2003**, *42*, 8870−8878.
(61) Periquet, M.; Fulga, T.; Myllykangas, L.; Schlossmacher, M. G.; Feany, M. B. *J. Neurosci.* **2007**, *27*, 3338−3346.
(62) Rodriguez, J. A.; Ivanova, M. I.; Sawaya, M. R.; Cascio, D.; Reyes, F. E.; Shi, D.; Sangwan, S.; Guenther, E. L.; Johnson, L. M.; Zheng, M.; Jiang, L.; Arbing, M. A.; Nannenga, B. L.; Hattne, J.; Whitelegge, J.; Brewster, A. S.; Messerschmidt, M.; Boutet, S.; Sauter, N. K.; Gonen, T.; Eisenberg, D. S. *Nature* **2015**, *525*, 486−490.
(63) Atsmon-Raz, Y.; Miller, Y. *J. Phys. Chem. B* **2015**, *119*, 10005−10015.
(64) Dettmer, U.; Newman, A. J.; Soldner, F.; Luth, E. S.; Kim, N. C.; Von Saucken, V. E.; Sanderson, J. B.; Jaenisch, R.; Bartels, T.; Selkoe, D. *Nat. Commun.* **2015**, *6*, 7314.
(65) Dettmer, U.; Newman, A. J.; Von Saucken, V. E.; Bartels, T.; Selkoe, D. *Proc. Natl. Acad. Sci. U. S. A.* **2015**, *112*, 9596−9601.

DOI: 10.1021/jacs.5b13261
J. Am. Chem. Soc. 2016, 138, 4458−4467

(66) Cleary, J. P.; Walsh, D. M.; Hofmeister, J. J.; Shankar, G. M.; Kuskowski, M. A.; Selkoe, D. J.; Ashe, K. H. *Nat. Neurosci.* **2005**, *8*, 79−84.

(67) ^{1}H NMR and DOSY studies of peptide **1a** at 50−250 μM indicated that peptide **1a** is monomeric and unstructured. At higher concentrations in the presence of buffers, peptide **1a** precipitates. These experiments in conjunction with the CD experiments suggest that peptide **1a** is unstructured in aqueous solution but folds under the crystallization conditions and in the presence of anionic lipids.

DOI: 10.1021/jacs.5b13261
J. Am. Chem. Soc. 2016, 138, 4458−4467